THE ASTROPHYSICAL JOURNAL, 334:746–760, 1988 November 15

MERIDIONAL CIRCULATION AND THE LITHIUM ABUNDANCE GAP IN F STARS

PAUL CHARBONNEAU AND GEORGES MICHAUD[1]
Département de Physique, Université de Montréal
Received 1988 February 4; accepted 1988 April 27

ABSTRACT

The effect of meridional circulation on the time evolution of superficial abundances of helium, lithium, and beryllium in F stars is calculated in detail. It is shown that, as long as the presence of convection zones is assumed not to modify global meridional circulation patterns, the maximum equatorial rotational velocity allowing the settling of Li and He decreases rapidly with $T_{\rm eff}$, going from 50 km s^{-1} at 7250 K to only 5 km s^{-1} at 6400 K. This is due to the rapid deepening of the superficial convection zone. Calculations also show that meridional circulation reduces considerably any overabundance of lithium produced by radiative acceleration.

It is also shown that, for stars of the age of the Hyades with $T_{\rm eff} < 7000$ K and rotational velocities larger than $\sim$25 km s^{-1}, meridional circulation is rapid enough to bring to the surface matter that originally was deep enough to have been depleted of its Li through nuclear burning. Lithium underabundances are then expected to appear at the surface. However, for rotational velocities up to 50 km s^{-1}, slight overabundances would be expected for $T_{\rm eff} > 7000$ K, since the radiative acceleration should be able to shield the surface Li from transport by circulation and subsequent destruction. This transport process leads to a possible explanation of the Li abundance gap observed in the F stars of the Hyades and other open clusters.

Observational tests are suggested to distinguish between this scenario and the gravitational settling model or turbulent diffusion model. In particular, it is shown how the Li/Be ratio varies in the presence of transport by meridional circulation. More observations of Be are needed in order to constrain the models.

Because of its simplicity, a preference is expressed for the gravitational settling model. Whichever model is eventually confirmed by observations, it is clear that light-element abundances can supply important constraints to hydrodynamical processes in stellar envelopes, meridional circulation, and turbulence in particular.

Subject headings: clusters: open — diffusion — stars: abundances — stars: evolution — stars: interiors — stars: rotation

I. INTRODUCTION

It has recently been shown (Charbonneau and Michaud 1988, hereafter CM) that meridional circulation prevents the gravitational settling of He in AmFm and HgMn stars when their rotational velocity is larger than about 90 km s^{-1}. This agrees with the maximum rotational velocity measured in these objects and so can be interpreted as a successful test of the meridional circulation model of Tassoul and Tassoul (1982, hereafter T^2), which was used in these calculations. One can, however, ask what happens as convection zones (CZs) become deeper with decreasing $T_{\rm eff}$. One of us has suggested (Michaud 1986) that in early F stars gravitational settling caused the Li abundance gap first observed in the Hyades. Is this explanation also consistent with the meridional circulation model of T^2? Superficially one may expect that it is, since the maximum observed rotational velocity of stars located in the Li gap is 50 km s^{-1}, a factor of 2 smaller than the maximum rotational velocity observed for the FmAm and HgMn stars. Applying to F stars the results of CM leads one to expect that meridional circulation is too slow to stop chemical separation. The situation is actually more complex. The critical rotational velocity allowing settling turns out to depend on the mass of the convection zone, which, in the range of mid-F dwarfs, increases rapidly as $T_{\rm eff}$ decreases. Furthermore, circulation not only influences the settling of Li; it can also bring to the surface matter originally located at depths where Li is promptly destroyed by nuclear reactions. The Li abundances in F stars turn out to be a very sensitive test of meridional circulation models.

The rather abrupt deepening of the superficial convection zones as $T_{\rm eff}$ decreases below 7000 K leads to an interesting question relating to the hydrodynamics of F stars: to what extent does meridional circulation penetrate the convection zone? The outer boundary condition to use for meridional circulation becomes uncertain, since the calculations of T^2 assume a completely radiative outer zone, and it is not clear how the presence of a relatively massive convection zone (up to 10^{-3} in mass) might affect their results. One could argue that meridional circulation is not needed within the convection zone to balance the radiative flux and thus that the velocity field is essentially that obtained for a purely radiative model, but treating the bottom of the convection zone as the outer boundary. One could equally well argue, as we did for the shallow superficial CZs of FmAm and HgMn stars (10^{-9} to 10^{-10} in mass), that the global meridional circulation pattern is not essentially modified by the presence of superficial convection zones; the only effect on particle transport would then amount to an averaging of abundances over the convection zone.

The recent high-quality observations of Li in a number of open clusters offer a unique opportunity to use F stars to test many of these hydrodynamical assumptions. Data have accumulated (see Fig. 1) showing that the lithium abundance gap first observed in Hyades F stars (Boesgaard and Tripicco 1986*a*) is a common feature of clusters old enough to have

[1] Killam Foundation Fellow.

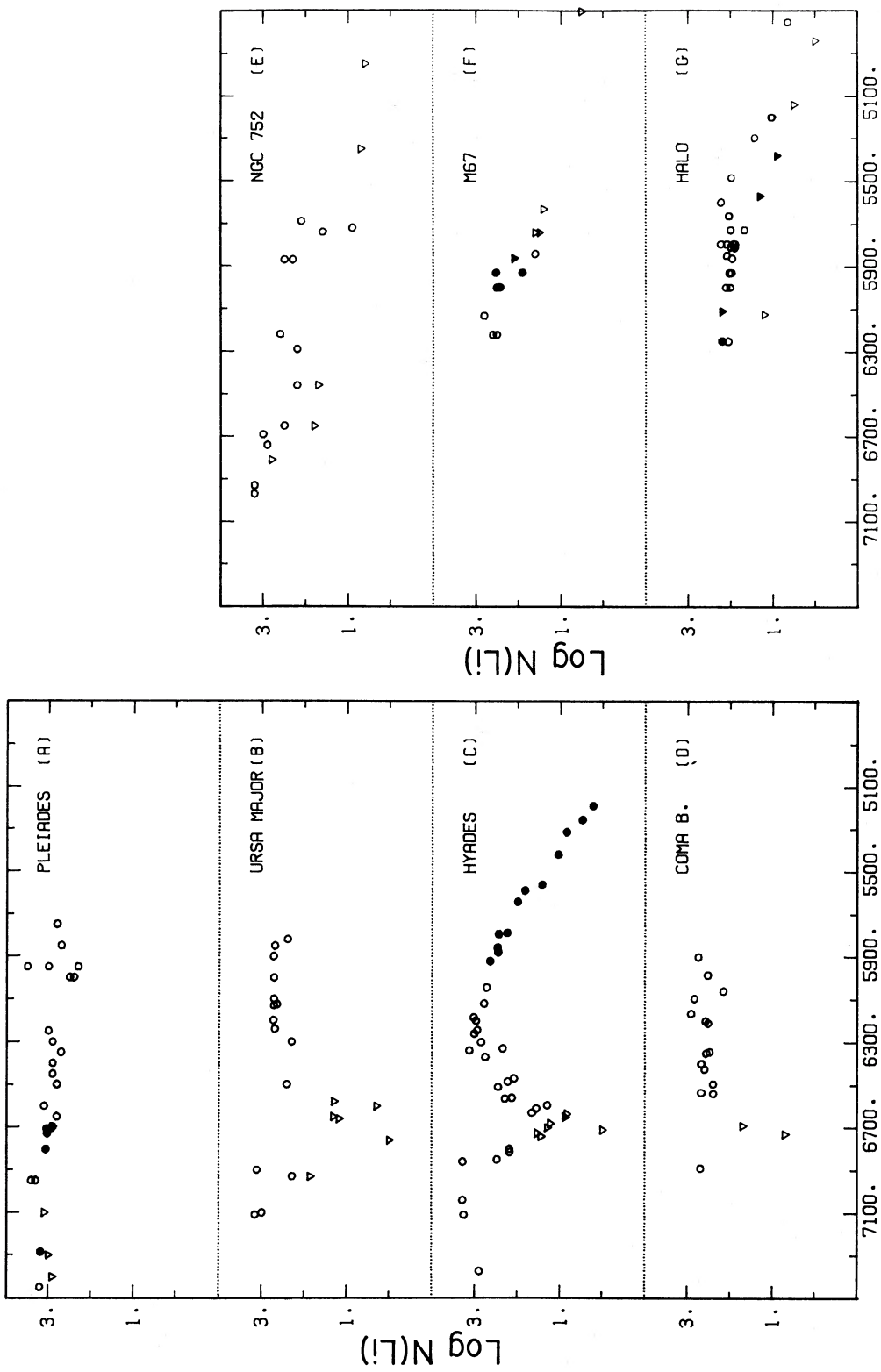

FIG. 1.—Lithium abundance vs. observed effective temperature in open clusters. Circles represent measured values, and triangles upper limits. Hyades data are taken from Boesgaard (1987*b*; *open symbols*) and Cayrel *et al.* (1984; *filled symbols*). The data from Ursa Major, Coma, and NGC 752 are taken respectively from Boesgaard, Budge, and Burck (1988), Boesgaard (1987*a*), and Hobbs and Pilachowski (1986*a*). Pleiades data are taken from Pilachowski, Booth, and Hobbs (1987; *open symbols*) and Boesgaard, Budge, and Ramsay (1988; *filled symbols*, for the stars not included in the Pilachowski, Booth, and Hobbs sample). M87 data are taken from Hobbs and Pilachowski (1986*b*; *open symbols*) and Spite *et al.* (1987; *filled symbols*). Data for halo stars are also shown, taken from Spite, Maillard, and Spite (1984; *open symbols*) and Hobbs and Duncan (1987; *filled symbols*, for stars not present in the Spite *et al.* sample).

developed the gap while still having basically unevolved F stars of the appropriate $T_{\rm eff}$. This gap, though not as well defined as in the Hyades, is present in the Coma (Boesgaard 1987*a*) and UMa (Boesgaard, Budge, and Burck 1988) clusters. It is not seen in the Pleiades (Pilachowski, Booth, and Hobbs 1987; Boesgaard, Budge, and Ramsay 1988), which was to be expected in view of the small age of this cluster. In the older clusters NGC 752 (Hobbs and Pilachowski 1986*a*) and M67 (Hobbs and Pilachowski 1986*b*; Spite *et al.* 1987), all stars in the gap and cooler seem to have had their Li abundance reduced from the initial value log $N(\rm Li) = 3.0$ [as measured on a scale where $N(\rm H) = 10^{12}$]. This is consistent, at least qualitatively, with the abundance evolution to be expected from the settling of Li coupled with burning by turbulent transport in cooler stars. These two processes, acting simultaneously, would cause the gradual disappearance of the $T_{\rm eff}$ interval between 6000 and 6400 K, where Li has apparently its initial value (see Figs. 1*d* and 1*e*). This suggests that in the older halo stars the Li abundances in this temperature range are *not* equal to the initial (cosmological) value. A proper understanding of processes involved is needed if we are to determine the true cosmological Li abundance from Li abundances observed in old halo stars (Michaud, Fontaine, and Beaudet 1984).

In the UMa moving group and in the new study of the Hyades, Boesgaard, Budge, and Burck (1988) and Boesgaard (1987*b*) obtain in some stars upper limits of 10^{-3} with respect to the original Li abundance. Since equivalent width measurements are uncertain by ± 2 mÅ for those relatively rapid rotators (Boesgaard, Budge, and Burck 1988, § II). and since an underabundance by a factor of 30 leads to an equivalent width of about 2 mÅ in the middle of the gap (see Fig. 4 of Boesgaard and Tripicco 1986*a*), it appears to us that underabundances by factors of more than 30 are extremely difficult to measure and would require confirmation. The presence of a blend can only make the determination of the upper limit even more difficult, and cannot be used to decrease the upper limits, as Boesgaard, Budge, and Burck (1988) have apparently done.[2]

We shall consider four effective-temperature intervals, in which the physical processes responsible for the Li abundance variations are different or operate with different time scales. The first includes stars with $T_{\rm eff} < 6000$ K, where nuclear burning of Li is involved (Schatzman 1977; Vauclair *et al.* 1978; Baglin, Morel, and Schatzman 1985; Michaud 1985). The second spans the range $6400 > T_{\rm eff} > 6000$ K. In stars younger than $\sim 10^9$ yr, this is too cold for gravitational settling to have affected Li abundances and too warm for whatever process destroying Li in G and K dwarfs to have had a measurable effect. The third covers the interval 6400–6900 K, where gravitational settling is potentially important, and the fourth groups all stars with $T_{\rm eff} \geq 6900$ K, whose abundance evolution is expected to be strongly influenced by radiative acceleration.

It is especially important to study meridional circulation in these objects, since rotation has been suggested to play a dominant role in the existence of the Li abundance gap. Noting that, at least in the Hyades, rotational velocities of the stars in the Li gap are generally larger than that of cooler stars, Boesgaard (1987*b*) suggested that it could well be that rotation plays an essential role in the appearance of this feature.

One might gain more insight by examining the data in the $T_{\rm eff}$–v sin i plane, which is done in Figure 2. Filled squares correspond to stars with log $N(\rm Li) \geq 2.5$, dotted squares to $2.5 >$ log $N(\rm Li) \geq 1.5$, and open squares to log $N(\rm Li) < 1.5$. The following points should be made. First, the rather sharp drop in v sin i with decreasing $T_{\rm eff}$ known to exist in mid-F dwarfs (see, e.g., Abt 1970) is clearly apparent here. Second, all Li-deficient stars fall in a narrow effective-temperature interval centered around 6700 K. Third, some stars with both high N(Li) and high v sin i can be found in the samples; actually, more than half the Li-normal stars on the high-$T_{\rm eff}$ side of the gap have large v sin i. This suggests that rotation may have little to do with the appearance of the gap, and that the apparent N(Li)–v sin i correlation seen in the Hyades could be an

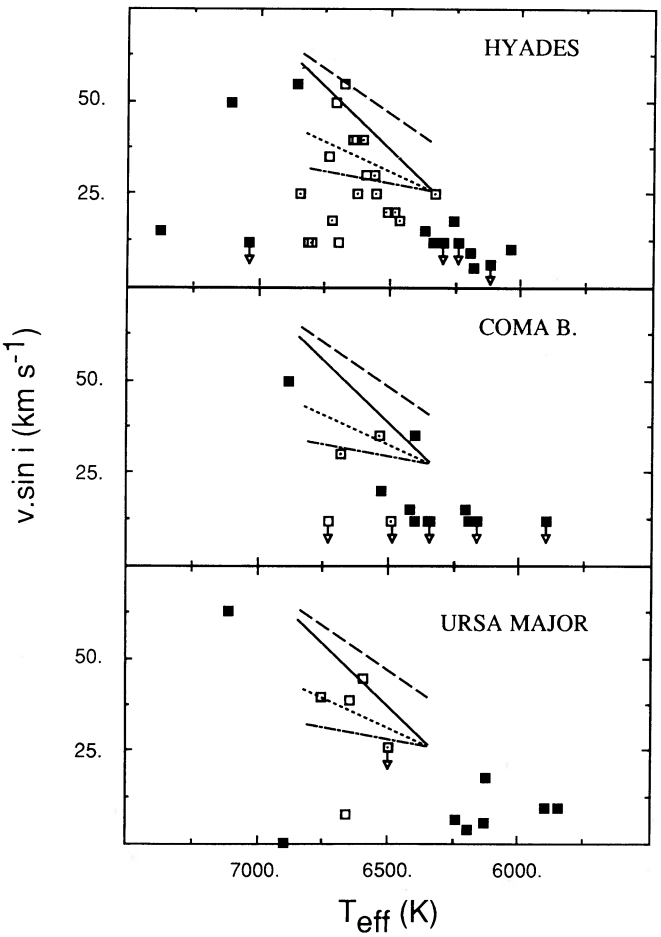

FIG. 2.—Lithium abundances in the $T_{\rm eff}$–v sin i plane, for some samples of Fig. 1 for which accurate values of v sin i are known. Filled squares represent stars having log $N(\rm Li) \geq 2.5$, dotted squares correspond to $2.5 >$ log $N(\rm Li) \geq 1.5$, and empty squares to log $N(\rm Li) < 1.5$. The sharp drop in average v sin i as $T_{\rm eff}$ decreases is obvious for all three clusters. Note how, in all samples, some Li-rich stars with both high v sin i and high $T_{\rm eff}$ can be found. Similarly, Li-poor stars, with small v sin i, are found in the middle of the gap. The various straight lines are *not* attempted fits, but rather refer to calculations of § V.

[2] After this paper was written, Boesgaard and Budge (1988) and Boesgaard (1988, private communication) kindly carried out a more conservative estimate of the upper limits to the Li abundance in the Hyades, UMa, and Coma clusters. They reconsidered all but one of the stars with upper limits corresponding to underabundances by more than a factor of 50. Among the stars reconsidered, there now remains none with upper limits implying underabundances by more than a factor of 50.

artifact of the aforementioned $v \sin i$–$T_{\rm eff}$ reationship for main-sequence stars. It should also be mentioned that Balachandran, Lambert, and Stauffer (1987) and Balachandran (1987) find that the late F, G, and K dwarfs of the young cluster α Persei (age $\approx 5 \times 10^7$ yr) with rotational velocities larger than 50 km s^{-1} have high Li abundances, while stars rotating more slowly show smaller Li abundances.

It is also possible to evaluate any correlation between rotational velocity and Li underabundance by comparing average values of rotational velocity for groups of stars with different Li abundance. This is done separately for field and cluster stars in Table 1. Two groups are defined: stars in the gap ($6500 < T_{\rm eff} < 6800$ K) and stars with apparently the original abundance in clusters younger than 10^9 yr, with $6000 < T_{\rm eff} < 6400$ K. The apparent rotational velocity dependence of Li underabundance, as seen in Figure 2, also appears in the cluster data of Table 1. The hotter cluster stars with $\log N(\rm Li) < 1.5$ have an average rotational velocity which is larger than that of any of the other groups. In the cooler stars there are no objects with $\log N(\rm Li) < 1.5$, but stars with $1.5 < \log N(\rm Li) < 2.5$ have a rotational velocity that appears significantly larger than those where Li is more nearly normal. This correlation is, however, inconsistent with averages for field stars. Since there are more field stars than cluster stars, one would expect the correlation to be more clearly present. However, no correlation at all is seen in field stars. Among the hotter objects, the slower-rotating ones are also the most Li-deficient, but this correlation is absent in cooler objects. Although variations in average rotational velocities between the different groups of objects are of the same order for cluster and field stars, the latter show no correlation between rotational velocities and Li abundances. This then suggests that the correlation seen in clusters may well not be real. Our analysis on field stars contradicts that of Thévenin, Vauclair, and Vauclair (1986), presumably because they used a smaller sample (note that all stars of Thévenin *et al.* are included in our sample). There could also be selection effects affecting the determination of these averages, since, for instance, Doppler broadening in rapidly rotating stars makes the measurement of small equivalent widths impossible, generally yielding only upper limits on Li abundances.

Potential relations between diffusion and meridional circulation must, however, be fully explored. Accordingly, we successively study in this paper the settling of He in the presence of meridional circulation (§ II) in order to understand (1) the link with the FmAm stars and (2) how the FmAm phenomenon disappears in the cooler stars. In parallel, the Li settling velocity is calculated and compared with the He settling velocity in order to determine the maximum rotational velocity allowing the Li abundance gap to develop, if the meridional circulation velocity field is given as calculated by T^2. The effect of circulation on diffusion caused by the combined effects of radiative acceleration and gravity is then studied in detail (§ III), in order to determine whether or not meridional circulation can replace mass loss as the phenomenon reducing expected Li overabundances above $T_{\rm eff} = 6900$ K. The possibility that meridional circulation causes a decrease in Li abundances by bringing Li-depleted material to the surface is also studied in detail (§ IV). Finally, comparisons with observations are made in § V, an alternative model to explain the Li gap is developed, and observational tests are suggested to distinguish between the different hydrodynamical possibilities.

TABLE 1

AVERAGE $v \sin i$ IN FIELD AND CLUSTER STARS[a]

log N(Li)	$6000 < T_{\rm eff} \leq 6400$ K	$6500 < T_{\rm eff} \leq 6800$ K
	Field Stars	
>2.5	11 (3)	18 (16)
1.5–2.5	16 (17)	21 (8)
<1.5	11 (17)	12 (6)
	Cluster Stars	
>2.5	11 (17)	20 (1)
1.5–2.5	19 (2)	28 (8)
<1.5	... (0)	34 (12)

[a] Average values are given in km s^{-1}. The number in parentheses next to each entry indicates how many stars are included in the corresponding subgroup.

II. HELIUM SETTLING AND MERIDIONAL CIRCULATION IN F STARS

Calculations on the diffusion of He in F stars in the presence of meridional circulation were performed, using the two-dimensional technique described in some detail in CM. It uses an algorithm developed by Pelletier (1986), based on the "box method" of Keller (1974). Given a three-dimensional grid (two spatial dimensions plus time), it yields abundance values at any point (r, θ) of the envelope, as a function of time. Complete mixing is imposed after each time step within the superficial convection zones. The meridional circulation velocity field is taken from T^2. Their Table 9 is used, corresponding to Kramers's opacity and $q = 6$ (i.e., the turbulent viscosity is taken as $10^6\ \mu_r$, μ_r being the usual radiative viscosity).

Model envelopes were produced using Martel's (1974) implementation of a Paczyński envelope code. All models have $\log g = 4.3$ and solar abundances, and span the interval $7250 \geq T_{\rm eff} \geq 6300$ K. Values in the range $1.0 \leq \alpha \leq 2.0$ were used for α, the ratio of mixing length to pressure scale height. Diffusion coefficients were taken from Paquette *et al.* (1986). As in the more massive models studied by CM, when meridional circulation is present, the He abundance in the CZ first decreases with time, but eventually levels off to a constant value that depends on the equatorial rotational velocity (v_e). One can thus determine, for any given stellar model, a critical v_e above which the He abundance in the CZ never decreases enough for the CZ to disappear [a factor of about 2.5 below the original abundance, assumed here to be N(He)/N(H) = 0.1]. CM have argued that the key parameter in determining the value of this critical rotational velocity is the ratio of diffusion to circulation velocities at the base of the CZ. In the effective-temperature range considered here, it turns out that the dependence on both α and $T_{\rm eff}$ can be parameterized by a single quantity, the convection zone depth. Figure 3*a* presents the critical v_e allowing disappearance of the superficial He CZ as a function of the CZ's depth. The curve was constructed by determining the critical v_e for each model of the sequence described above. The diffusion time scales vary enormously in this range. Figure 3*b* gives the time required for the He abundance in the CZ to fall a factor of 2 under the initial (cosmological) value. One can see that for shallow CZs the time scale is rather short, while the critical v_e is relatively large.

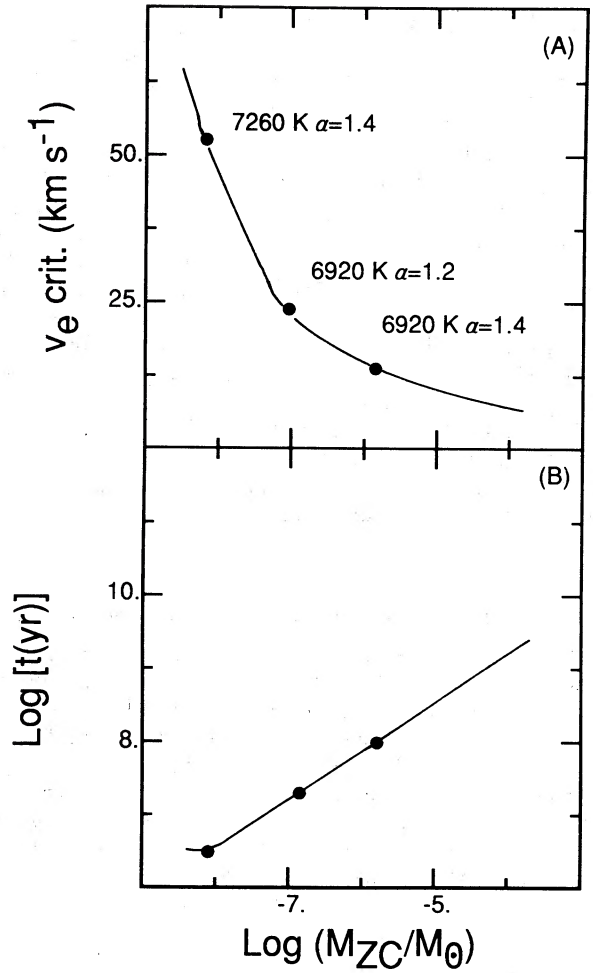

FIG. 3.—He settling in presence of meridional circulation in F stars. (*a*) Critical velocity above which the He CZ abundance will never fall below a factor of 2.5 under the initial (cosmological) value, the level at which the He superficial CZ disappears. (*b*) The corresponding time scales, defined here as the time required for the He abundance to fall a factor of 2 under the initial value. Stellar models are parameterized according to the CZ mass fraction. The locus of three models is indicated on each curve.

For the more massive CZs the critical v_e values fall below 10 km s^{-1}, but the time scales increase logarithmically.

Using Figure 2 of Michaud (1986), the reader can determine the depth of convection zones for different values of $T_{\rm eff}$ and α. For $\alpha = 1.4$, one finds that the limiting rotational velocity varies from 100 km s^{-1} at $T_{\rm eff} = 9000$ K (CM) to 50 km s^{-1} at $T_{\rm eff} = 7250$ K, 15 km s^{-1} at $T_{\rm eff} = 7000$ K, and 5 km s^{-1} at $T_{\rm eff} = 6400$ K. Thus, for $T_{\rm eff} < 6800$ K, only very slow rotators could develop He underabundances in the framework of the T^2 circulation model.

The physical reason for the rapid decrease of the critical rotational velocity as $T_{\rm eff}$ decreases can be traced to the variation of diffusion and circulation velocities as a function of depth in the star. Whereas the vertical component of the circulation velocity, outside the surface boundary layer, varies very slowly as depth increases, the gravitational settling velocity varies as $T^{1.5}/N$ (N being the proton density), leading to a decrease of the ratio of settling to circulation velocities. Although above 7500 K the depth of the surface He convection zone shows relatively little dependence on $T_{\rm eff}$, it increases rapidly below 7500 K, leading to a rapid decrease of the critical velocity.

Figure 4 shows He abundance evolution curves, for models having $T_{\rm eff} = 6918$ K and for various values of α. The horizontal dashed line indicates depletion by a factor of 2.5, the level at which the superficial He CZ is expected to disappear. Full curves correspond to nonrotating models, dotted curves to models with $v_e = 15$ km s^{-1}. Only settling is included here, and nonlinear terms were neglected (see CM). Since increasing α increases the depth of the convection zone and thus its total mass, it leads to larger settling times and smaller critical rotational velocities. This shows how sensitive the results are to α. Abundance evolution curves for Li would almost coincide with those of He. This may appear surprising, but one can actually verify that, in the effective-temperature range corresponding to mid-F dwarfs, the gravitational settling velocities at the base of the CZ are nearly identical for He and Li (3.00×10^{-7} and 2.92×10^{-7} cm s^{-1}, respectively, at 6918 K, $\alpha = 1.4$). *For $T_{\rm eff} < 6800$ K, gravitational settling is thus able to produce large* Li *underabundances only in the slowest rotators.*

III. RADIATIVE FORCES ON LITHIUM AND MERIDIONAL CIRCULATION

Michaud (1986) has shown that the presence of the lithium abundance gap observed in the Hyades F stars (Boesgaard and Tripicco 1986*a*) could be explained by competition between gravitational settling and radiative forces. The fact that he could reproduce the position and width of this gap without any arbitrary parameter is a strong argument in favor of the impor-

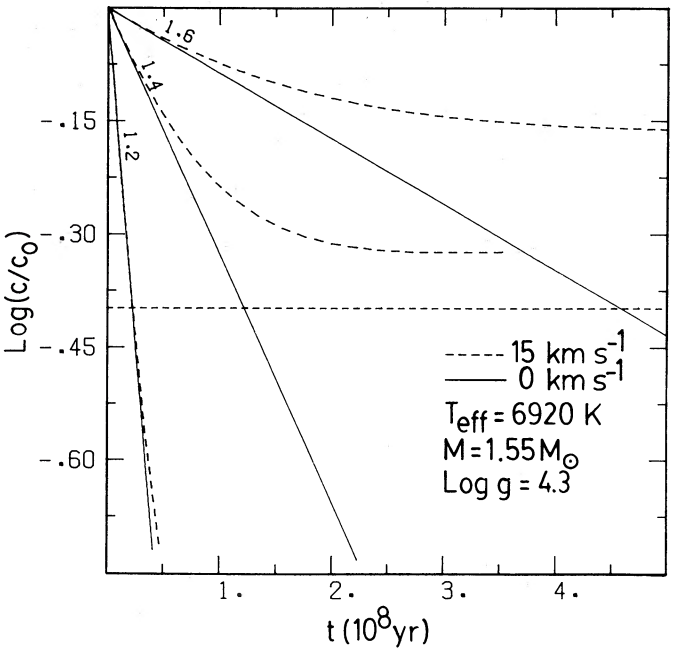

FIG. 4.—Abundance evolution of He for nonrotating models (*solid lines*) and $v_e = 15$ km s^{-1} (*dashed lines*). The horizontal dashed line indicates depletion by a factor of 2 from the initial concentration. The models used here all have $T_{\rm eff} = 6920$ K, $M = 1.55\ M_\odot$, and $\log g = 4.3$. Curves are labeled according to the value of α that was used in each case. Abundance evolution curves for Li would almost coincide with those shown here, settling velocities for Li and He being nearly identical at the base of the CZ for stars in this effective temperature range.

tance of diffusion in F stars. Since meridional circulation has been shown to be capable of greatly influencing gravitational settling, it can be expected that it will also have an effect on upward diffusion driven by radiative forces, and may decrease the expected Li overabundances obtained by Michaud (1986) for $T_{\rm eff} > 7000$ K.

To treat this problem, one merely includes in the diffusion velocity equation a suitable radiative acceleration term. The expression becomes

$$w = D_{13}\left(-\nabla \ln c + (1 - 2A + Z)\frac{m_p g}{2kT}\hat{r} + A\frac{m_p g_R}{kT}\hat{r}\right). \quad (1)$$

The quantity c is the concentration, a function of both r and θ, D_{13} is the diffusion coefficient of Li in H, taken from Paquette *et al.* (1986), and g_R is the radiative acceleration on Li, taken from Michaud (1986). For a discussion of the uncertainties in g_r see Vauclair (1987). Other symbols have their usual meanings. Upon inserting this expression in the continuity equation, one obtains a second-order, time-dependent, parabolic partial differential equation, exactly similar in structure to that arising from gravitational settling. The method of CM, briefly discussed in § II, is therefore suitable.

Numerically, it turns out that Li diffusion with radiative acceleration is more difficult to treat than that of He (or Li) settling. This is because the radiative acceleration introduces a very sensitive dependence of the total diffusion velocity on temperature (i.e., on depth). Figure 5 shows the total diffusion velocity (settling + radiative terms) as a function of depth ($\Delta M/M$). The model used here has $M = 1.6\ M_\odot$, $T_{\rm eff} = 7000$ K, and $\log g = 4.3$. The short dotted lines on the horizontal axis indicate the position of the bottom and top of the CZ, for various values of α. Within the CZ, the precise value of w is unimportant, since convective motions will smooth out any abundance gradient established by diffusion. Even when meridional circulation is turned off, the steep velocity gradient located near $\Delta M/M \approx 10^{-5}$ generates undamped oscillations in the abundance profile if a standard radial mesh is used. It was found necessary to use an adaptive mesh, concentrating zones in regions of high velocity gradients. The large velocities near the stellar surface also proved difficult to handle. Calculations were therefore performed only up to the top of the He superficial CZ. Neglecting the mass above, amounting to about 0.1% or less of the CZ's mass, is not expected to introduce appreciable errors in the final results.

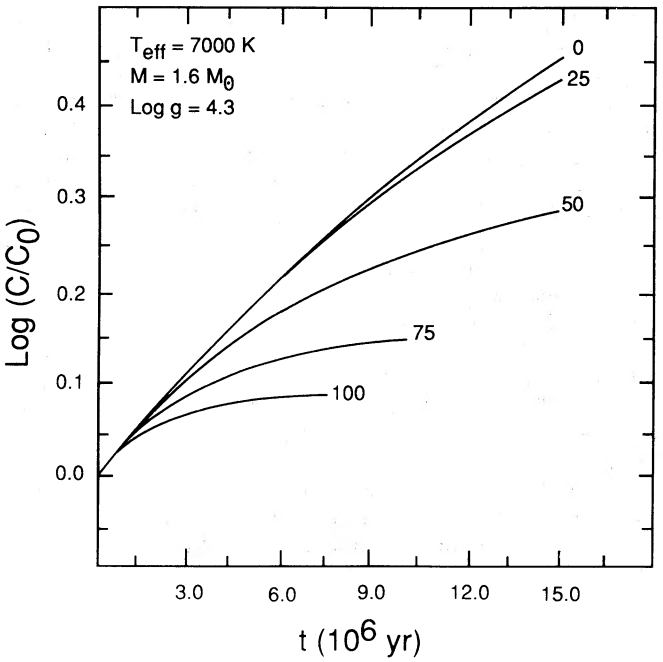

FIG. 6.—Li abundance evolution curves for a model with $T_{\rm eff} = 7000$ K, log $g = 4.3$, $M = 1.6\ M_\odot$, and $\alpha = 1.4$. The curves are labeled according to the various equatorial rotational velocities used, in kilometers per second. Radiative acceleration is included in the diffusion velocity calculation, along with gravitational settling. Circulation can greatly reduce the overabundances that radiative acceleration would otherwise lead to.

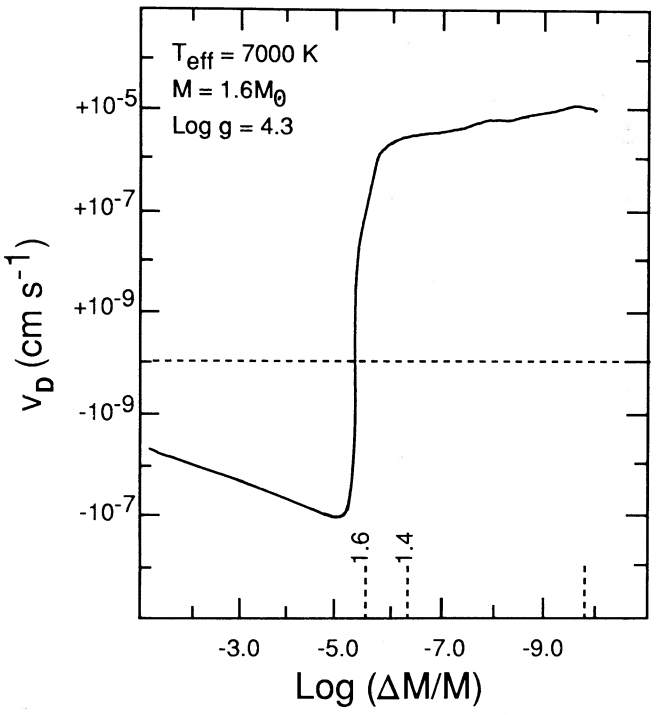

FIG. 5.—Total diffusion velocity (i.e., gravitational plus radiative terms) as a function of the mass above the point of interest (model with $T_{\rm eff} = 7000$ K, log $g = 4.3$ and $M = 1.6\ M_\odot$). The short-dotted lines on the horizontal axis indicate positions of the bottom and top of the superficial He CZ, for various values of α as indicated. Note the peculiar vertical scale (linear between -10^{-9} and $+10^{-9}$; otherwise logarithmic).

Some *a priori* knowledge regarding Li abundance evolution can already be extracted from Figure 5. Since the total diffusion velocity is upward-directed at the CZ's base, Li overabundances are expected to develop in the CZ. Note that these will not increase indefinitely, since the reservoir of available Li is not so large (Li sinks under $\Delta M/M \approx 4 \times 10^{-6}$). The CZ's bottom being located here at $\Delta M/M \approx 5 \times 10^{-7}$, the maximum possible overabundance is by a factor of about 8, provided that all available Li is pushed up.

The effect on abundance evolution of the interaction between meridional circulation and diffusion when the radiative acceleration is greater than gravity is shown in Figure 6. It shows the time evolution of CZ Li abundances for the same model as in Figure 5, with various equatorial rotational veloc-

ities. Some curves extend to greater ages than others, since evolution was stopped at the onset of instabilities. The effect of convection on abundance profiles was simulated by averaging the abundances over the convection zone at each time step. Meridional circulation starts having large effects for rotational velocities larger than ~ 40 km s^{-1}, a factor of 3 larger than for gravitational settling (see Fig. 4). The difference comes partly from the higher $T_{\rm eff}$, yielding a shallower CZ, and from the fact that the radiative acceleration on Li is more than twice as large as the gravitational acceleration in this model. For $v_e = 0$ we have verified, by continuing the integration to 5×10^7 yr, that the abundance did eventually saturate at an overabundance factor of ~ 8, as expected. The maximum overabundance is only by about a factor of 2 at 50 km s^{-1}, and by a factor of ~ 1.2 at 100 km s^{-1}. Clearly, *meridional circulation induced by rotation can reduce overabundances expected from nonrotating models.*

It is instructive to look at the detailed space distribution of Li in the star in order to understand better the effect of meridional circulation on the abundance evolution, to study the competition between meridional circulation and diffusion, and also to detect the appearance of numerical instabilities. Four cases are shown; in Figure 7*a* the radial abundance profiles are shown for various epochs (labeled in units of 10^6 yr), in a nonrotating model. The progressive accumulation of Li in the convection zone can clearly be seen. The zone where Li is pushed upward is progressively emptied of its Li, and a deep hole in Li abundance forms. The smaller hole located deeper is due to pure gravitational settling. At later epochs, the rate of increase of the abundance of Li in the CZ decreases, as less and less Li remains available to be pushed upward. Instabilities can be seen in the solution at the end of the evolution, taking the form of steps in the abundance profiles, located slightly above the bottom of the hole. These do not appear to have significantly modified the solution, as conservation tests show that Li is conserved to better than 98% in the CZ. Figure 7*b* shows radial abundance profiles at the pole for the case $v_e = 25$ km s^{-1}. The abundance hole is still apparent, although it is not so deep. This was to be expected, since circulation tends to "fill" the hole from below, carrying to it Li-undepleted matter. Pro-

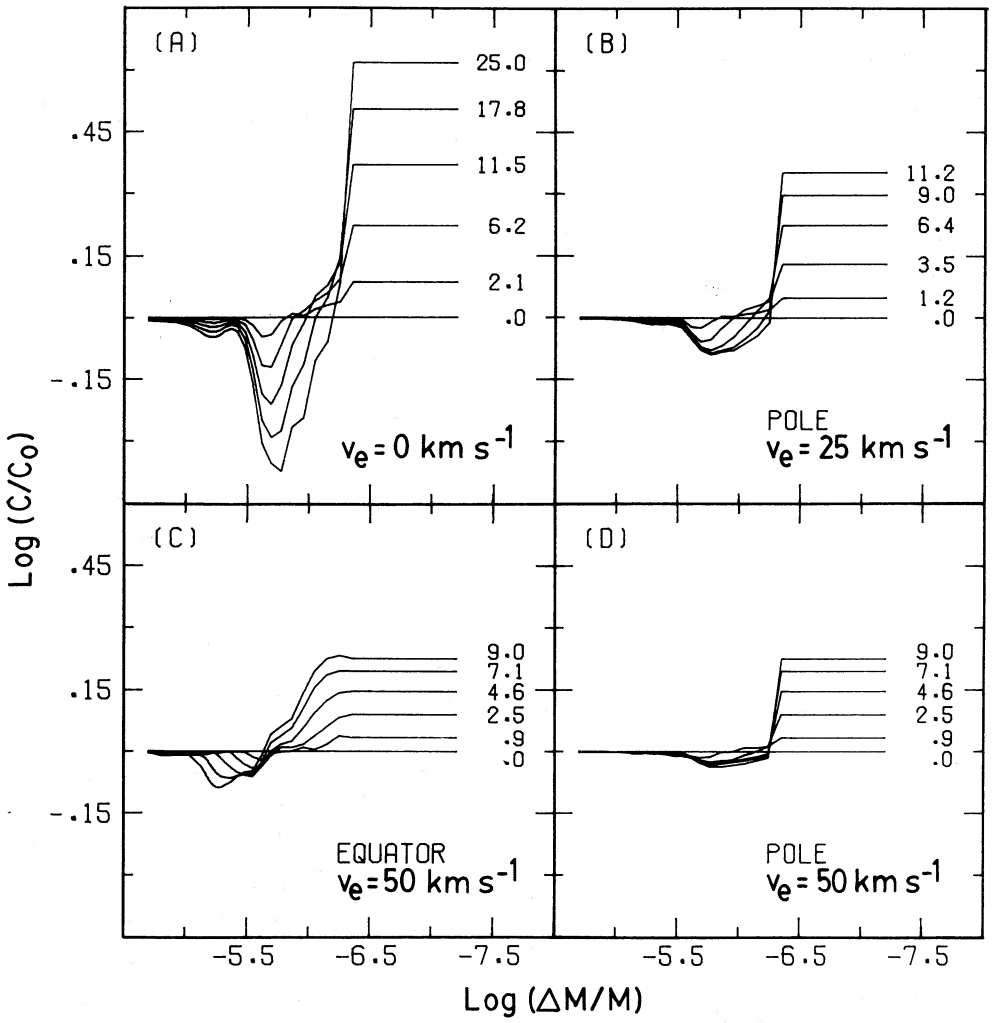

FIG. 7.—Li radial abundance profiles: (*a*) 0 km s^{-1}, spherically symmetric; (*b*) 25 km s^{-1}, pole; (*c*), (*d*) 50 km s^{-1}, equator and pole, respectively. The models used here are the same as in Fig. 6. Abundances in the CZ are averaged at each time step. The curves are labeled in units of 10^6 yr.

files at the equator (not shown) are practically identical with those for the nonrotating case. This is essentially because the downward-directed meridional circulation is still smaller (by a factor of ~ 3) than the upward-directed diffusion velocity. This leads to the same underabundance, at the lowest point of the abundance hole, as in the nonrotating case, but the hole is located at a slightly greater depth. The situation is, however, very different when $v_e = 50$ km s^{-1} (Fig. 7*c*). At the equator, the downward circulation velocity is then larger than the upward diffusion velocity, so matter is brought downward from the CZ, preventing the development of large underabundances immediately below it, contrary to the previous case. A Li abundance hole still forms, but it is of lesser depth and is located deeper in the envelope. Figure 7*d* shows abundance profiles at the pole for the same model. The abundance hole is nonexistent, since a mass element carried upward by the combined effect of radiative acceleration and circulation does not have time to lose any of its initial Li before completing the crossing of the hole region and being pushed up into the CZ.

The preceding calculations disregard the destruction of Li by nuclear reactions deeper in the envelope. It was explicitly assumed (in the form of the lower boundary condition in the diffusion calculation) that the Li abundance of matter arriving from below was equal to the cosmological value. After a certain time, this will, however, cease to be true, as matter that was originally located at depths where $T > 2.5 \times 10^6$ K starts arriving in the CZ. This effect is evaluated in the next section.

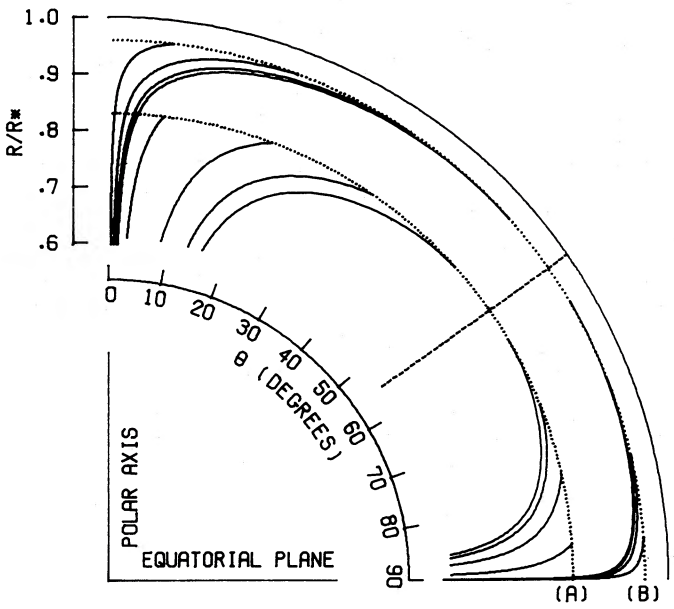

FIG. 8.—Streamlines of the meridional circulation velocity field of Tassoul and Tassoul (1982), for two stellar models of (*a*) 1.2 $M_\odot$ and (*b*) 1.6 $M_\odot$, corresponding to 6310 and 7000 K, respectively ($\alpha = 1.6$). Both models are normalized in radius. The dotted lines show the position of the CZ for each model. Only streamlines penetrating the convection zone are shown.

IV. LITHIUM BURNING VIA MERIDIONAL CIRCULATION

Basically, the situation is the following: in the polar regions, meridional circulation carries matter from regions where lithium is destroyed by nuclear burning (denoted by $r_{\rm Li}$, taken here as the depth at which $T = 2.5 \times 10^6$ K) to the bottom of the superficial He convection zone ($r_{\rm CZ}$). The large velocities associated with convective motions cause element mixing within the convection zone, on a time scale very much shorter than that of meridional circulation. The matter flowing out of the CZ in the equatorial region then has the same Li fraction as the CZ, and thus contains more Li than that entering in the polar region. The net effect of this process is thus to decrease the lithium abundance in the superficial convection zone. A kinematic method is developed in this section that makes it possible to follow the Li abundance evolution arising from this process. *Diffusion is here neglected.* The discussion presented in § V takes all processes into account.

Figure 8 shows meridional circulation streamlines for two stellar models, calculated from the velocity field derived by T^2. Only the streamlines entering the CZ are shown, since the others can play no role in the CZ abundance evolution. The integration along the streamlines starts at the depth $r_{\rm Li}$ discussed above. The velocity field is given by equations (117) of T^2:

$$U_r(r, \theta) = \tfrac{1}{2}\epsilon u(r)(3\cos^2\theta - 1)\,, \tag{2}$$

$$U_\theta(r, \theta) = -3\epsilon r v(r)\sin\theta\cos\theta\,, \tag{3}$$

with

$$\epsilon = \frac{\Omega_0^2 R_*^3}{GM_*} \propto v_e^2\,, \tag{4}$$

where v_e is the equatorial rotational velocity and R_* and M_* are the stellar radius and mass. The functions $u(r)$ and $v(r)$ are tabulated in T^2, for various values of turbulent viscosity and opacity. As in § II, Table 9 of T^2 is used (Kramer's opacity and $q = 6$). It turns out that the choice of q does not greatly influence the results presented later, since the meridional circulation solutions show a nonnegligible dependence on this parameter only near the surface and core boundary, outside the region of interest here. From equation (2), it is immediately obvious that at all depths U_r is maximal along the polar axis and decreases monotonically as θ increases, changing sign at $\theta_{\rm crit} \approx 55°$. Assigning an index i to each streamline, and denoting by t_i the time required to travel on that streamline from $r_{\rm Li}$ to $r_{\rm CZ}$, it is also obvious that

$$t_{i+1} > t_i\,, \quad i = 1, \ldots, i_{\rm crit}\,, \tag{5}$$

where $i_{\rm crit}$ corresponds to the last streamline capable of entering the CZ (at $\theta_{\rm crit}$). Calculating t_i amounts to evaluating the line integral

$$t_i = \int_{r_{\rm Li}}^{r_{\rm CZ}} \frac{\boldsymbol{U}\cdot d\boldsymbol{s}}{\boldsymbol{U}\cdot\boldsymbol{U}}\,, \tag{6}$$

where it is understood that the integration is performed along a given streamline. To evaluate equation (6), one assumes a starting position at $(r_{\rm Li}, \theta_i)$, calculates U_r and U_θ, chooses a small time interval dt, and then moves on the streamline by evaluating

$$\begin{aligned} r^{m+1} &= r^m + U_r(r^m, \theta^m)dt^m\,, \\ \theta^{m+1} &= \theta^m + U_\theta(r^m, \theta^m)dt^m\,. \end{aligned} \tag{7}$$

The exponent m indicates the time step. The dt's are chosen such as to satisfy a tolerance criterion of the kind

$$\max\left(\left|\frac{U_r^{m+1}-U_r^m}{U_r^m}\right|,\left|\frac{U_\theta^{m+1}-U_\theta^m}{U_\theta^m}\right|\right)\leq 10\%\ . \quad (8)$$

This process is repeated until the position r_{CZ} is reached. A convenient test can be derived from a well-known property of steady flows, that one and only one streamline is generated by a given value of the stream function (see, e.g., Landau and Lifshitz 1959, p. 22). Calculating the stream function at the beginning and end of the iteration shows immediately whether one has notably deviated from the initial streamline. For the flow described by equations (2) and (3), the stream function is given by equation (119) of T[2]:

$$\psi(r,\theta)=\tfrac{1}{2}\epsilon\rho r^2 u(r)\sin^2\theta\cos\theta\ . \quad (9)$$

In all calculations presented in this section, ψ_i remained constant within 10% during the whole iteration.

The average abundance in the CZ evolves in three distinct phases. At $t=0$ one has an initial concentration $c=c_0$ for $r>r_{Li}$, and $c=0$ deeper.[3] Since it takes a time $t_{i=0}$ before depleted matter starts entering the CZ on the fastest streamline, one has

$$\bar{c}(t)=c_0\ ,\quad 0\leq t\leq t_0\ . \quad (10)$$

The second phase then begins. Although matter entering the CZ on "slower" streamlines is still at concentration c_0, the contribution of the "faster" streamlines to the Li particle flux entering the CZ is now nil. Denoting by θ^m the angle corresponding, at t^m, to the last streamline on which one still has $c=c_0$ under the CZ, the surface-integrated particle flux into the CZ (i.e., the number of Li atoms entering the CZ per unit time, denoted by ϕ_e^m) can be written as

$$\phi_0^m=\frac{2}{m_p}\int_0^{2\pi}\int_{\theta_m}^{\theta_{\rm crit}} c_0\,\rho(r=r_{CZ})U_r(r=r_{CZ},\theta)dS$$
$$=\left.\frac{2\pi\epsilon u(r)r^2c_0\rho}{m_p}\right|_{r=r_{CZ}}[\cos\theta\sin^2\theta]_{\theta_m}^{\theta_{\rm crit}}\ ,\quad t_0<t\leq t_{i\,\rm crit}\ , \quad (11)$$

where equation (2) has been used to substitute for U_r, and the factor 2 multiplying the integral is needed to include contributions from both hemispheres. The angle $\theta_{\rm crit}$ is that at which the vertical component of the circulation velocity changes sign. The surface-integrated particle flux out of the CZ (ϕ_0^m) is simply calculated from the average concentration at the preceding time step:

$$\phi_0^m=\frac{2}{m_p}\int_0^{2\pi}\int_{\theta_{\rm crit}}^{\pi/2}\bar{c}^{m-1}\rho(r=r_{CZ})U_R(r=r_{CZ},\theta)dS$$
$$=\left.\frac{2.42\epsilon u(r)r^2\bar{c}^{m-1}\rho}{m_p}\right|_{r=r_{CZ}}\ ,\quad t_0<t\leq t_{i\,\rm crit}\ . \quad (12)$$

Knowing ϕ_e^m and ϕ_0^m, the average concentration in the CZ can be calculated:

$$\bar{c}^m=\bar{c}^{m-1}+\frac{m_p}{M_{CZ}}[\phi_e^m-\phi_0^m]\Delta t\ ,\quad t_0<t\leq t_{i\,\rm crit}\ , \quad (13)$$

where $\Delta t=t^m-t^{m-1}$, and M_{CZ} is the mass of the CZ.

The final phase begins when the flux into the CZ vanishes. It is easy to show that the abundance evolution is then described by the following analytical expression:

$$\bar{c}(t)=\bar{c}(t_{i\,\rm crit})\exp\left[-\lambda(t-t_{i\,\rm crit})\right]\ ,\quad t>t_{i\,\rm crit}\ , \quad (14)$$

$$\lambda=\left.\frac{2.42\epsilon u(r)r^2\rho}{M_{CZ}}\right|_{r=r_{CZ}}\ . \quad (15)$$

Equations (10), (13), and (14) describe the evolution of the Li abundance in the superficial convection zone of main-sequence stars, when the only process taken into account is the transport by meridional circulation of matter previously depleted of its Li by nuclear burning. The key parameters here are r_{Li} and r_{CZ}. Clearly the same method can be applied to the case of Be. One then merely starts the iteration at $r_{Be}=r(T=3.5\times10^6\ \rm K)$.

Figure 9 shows, as a function of $T_{\rm eff}$, the depths (measured in $\Delta M/M$ in Fig. 9*a* and in stellar radius units in Fig. 9*b*) where Li and Be burn, along with the position of the bottom of the CZ for various values of α. Figure 9*c* gives the t_0 values for Li (*dotted lines*) and Be (*dashed lines*) as defined by equation (6), again for various values of α. Figure 9*d* shows λ^{-1}, the *e*-folding time for phase 3 of the abundance evolution (cf. eq. [15]). The values of t_0 and λ given in Figure 9 were calculated assuming $v_e=1\ \rm km\ s^{-1}$; for other rotational velocities, the scaling goes as v_e^{-2} in both cases.

Figure 10 presents typical abundance evolution curves for Li and Be, as calculated from equations (10)–(15). The model has $M=1.2\ M_\odot$, $\alpha=1.6$, and $T_{\rm eff}=6310$ K. The dotted line gives the evolution of the n(Li)/n(Be) ratio. It should be noted that once Be enters the third phase of its abundance evolution, n(Li)/n(Be) remains constant, since both elements then flow out of the CZ at the same rate, which for a given v_e and model envelope depends only on the mass of the CZ and geometrical factors (cf. eq. [15]). The curves were calculated using $v_e=1\ \rm km\ s^{-1}$. It should be stressed that using a different v_e leaves the shape of the curves unchanged, and amounts merely to a redefinition of the time scales (i.e., of t_0 and λ).

V. DISCUSSION

a) Lithium Burning and Diffusion

In §§ II and III it was shown that meridional circulation can prevent element separation caused by diffusion both with and without radiative acceleration; how meridional circulation can directly lead to Li burning was studied in § IV. The combination of both processes can now be discussed. *This discussion assumes full penetration of the CZ by meridional circulation* (see § Ve below).

First, one may ask to what extent it is necessary to consider settling and burning together. As mentioned in § II and as can be obtained from Figure 3*a*, the critical rotational velocity for gravitational settling is about 15 km s^{-1} at $T_{\rm eff}=7000$ K, and falls to 5 km s^{-1} at $T_{\rm eff}=6400$ K (for $\alpha=1.4$). For stars rotating at these critical velocities, Li underabundances will be by a factor of 2.5 at most. For stars rotating faster, Li underabundances will evidently be smaller. The time scale for this depletion being a few times 10^8 yr, underabundances have plenty of time to appear in all clusters but the Pleiades. On the other hand, it is easy to obtain from Figure 9 the result that the critical velocity allowing Li burned material to start arriving in the CZ at the age of the Hyades is 20 km s^{-1}. Any star rotating

[3] Adopting such a steplike initial profile is a reasonable approximation, in view of the extreme sensitivity of the ^{7}Li(p, α)^{4}He reaction rate to temperature.

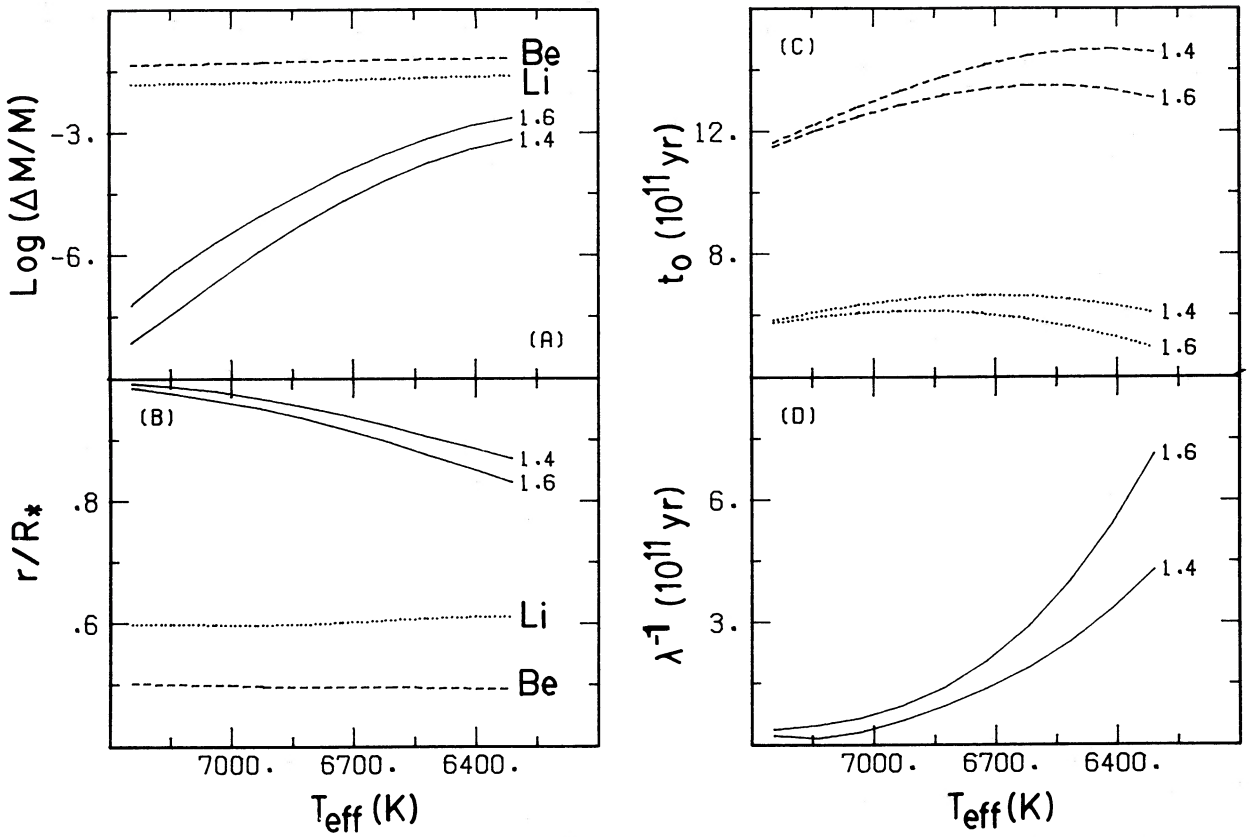

FIG. 9.—Transport of Li-depleted matter into the CZ by meridional circulation. (*a*, *b*) Positions, measured in mass fraction and stellar radius, respectively, corresponding to Li burning (*dotted line*), Be burning (*dashed line*), and the bottom of the superficial He CZ (*solid lines*, for two values of α). All models have $\log g = 4.3$. (*c*) Time required for Li- or Be-depleted matter to arrive in the CZ, for $\alpha = 1.4$ or 1.6, as defined in eq. (6), for $v_e = 1$ km s^{-1}. (*d*) Time scale of Li (or Be) depletion for the third phase of the abundance evolution, as defined by eq. (15).

faster will start to show some level of Li depletion due to transport by meridional circulation. The difference between 15 and 20 km s^{-1} is probably not significant, and it can be concluded that, at the age of the Hyades, all stars in the gap with $v_e \approx 20$ km s^{-1} are expected to have their Li abundance lowered by a factor of *at least* 2.5, the depletion being caused by diffusion *or* burning (via circulation). Those rotating more slowly are depleted in Li via gravitational settling, and those rotating more rapidly by burning via meridional circulation. On the other hand, at the age of the Hyades, the two processes do not lead to large effects simultaneously in the same star, and so can be considered separately. This becomes, however, less and less true as one considers clusters of increasing age, where both processes can have measurable effects in many stars.

The situation is somewhat different when radiative acceleration is considered. The effect of diffusion then remains important up to larger rotational velocities; as can be seen from Figure 6, it is only for velocities higher than about 40 km s^{-1} that the Li overabundance that diffusion first leads to in a 7000 K star starts to be significantly reduced. This is well above the critical velocity for Li-burned material to start arriving in the CZ at the age of the Hyades. One must then consider the two processes simultaneously. To this end, it is useful to define yet another critical velocity, which is the rotational velocity for which the total vertical transport velocity for Li is everywhere positive, that is, upward-directed. Since the circulation velocity is directed upward at the pole but downward at the equator (see Fig. 3*b* of Michaud 1987 for the angular dependence of the total transport velocity), this implies that if the (upward) diffusion velocity is larger than the (downward) circulation velocity at the equator, no Li can ever be carried out of the CZ by meridional circulation. This effectively shields the CZ from circulation. Even if matter depleted of its Li can eventually enter the CZ, no reduction in Li abundance can occur, since no Li can be carried out of it. This critical velocity for shielding is plotted in Figure 11 for $\alpha = 1.4$ and $\alpha = 1.6$. Up to this velocity, Li burning can lead to no Li underabundance in the CZ. Above that velocity, however, Li can eventually be carried out of the CZ by meridional circulation, thus yielding Li underabundances. In Figure 6, transport of Li-depleted material by circulation was neglected. This is a valid approximation up to 1.5×10^7 yr at $v_e = 50$ km s^{-1} (as shown in Fig. 6), since Li-burned material has not yet arrived under the CZ. The curves of Figure 6 can be extrapolated to longer times only as long as the rotational velocity is below the critical shielding velocity.

These results are particularly sensitive to the exact value of α used, as can be seen from Figure 11 and Figure 4. It has been argued that $\alpha = 1.9$ reproduced better the observed solar pulsations (Lebreton and Maeder 1986), although a value of $\alpha = 1.5$ is deduced from the position of the zero-age main sequence of the Hyades and other young clusters (VandenBerg and Bridges 1984). The larger values of α would imply that Li shielding could occur only in stars with effective temperatures

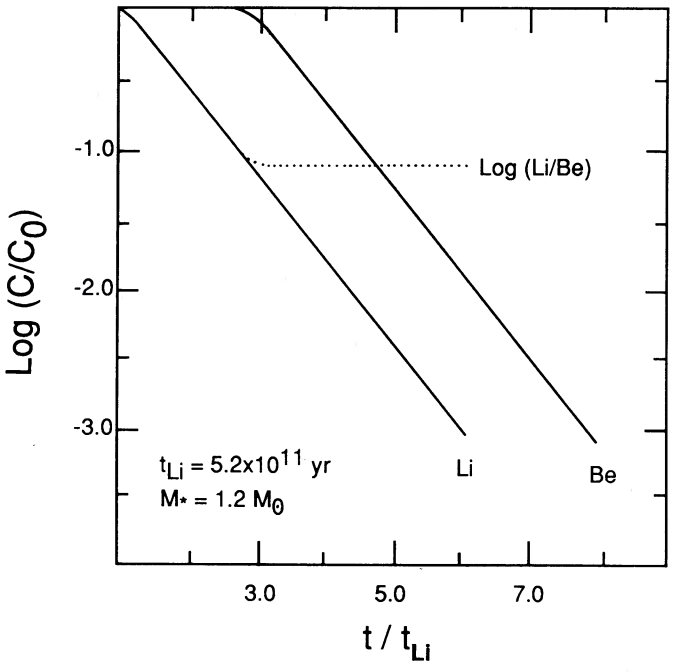

FIG. 10

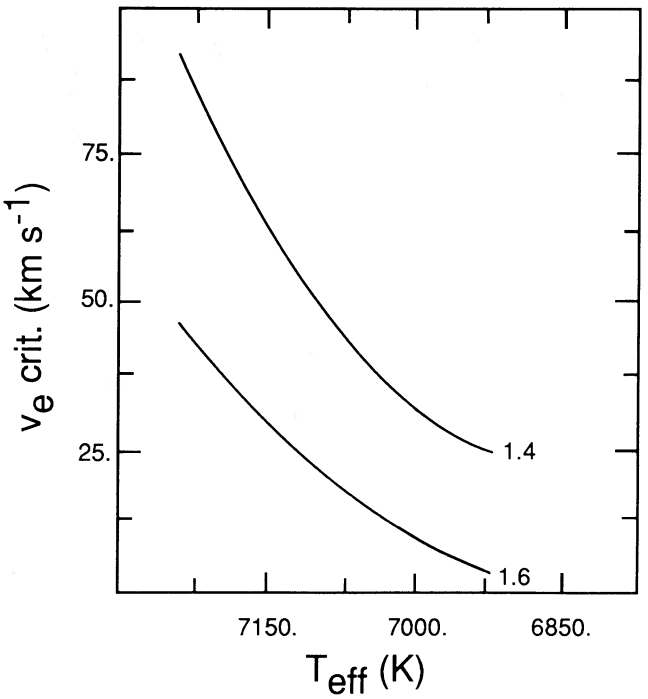

FIG. 11

FIG. 10.—Typical CZ abundance evolution curve caused by the burning of Li and Be via meridional circulation transport. The time evolution of the n(Li)/n(Be) ratio is also shown. The time (*abscissa*) is measured in units of $(t_0)_{Li}$, defined via eq. (6) as the time required for Li-depleted matter to reach the CZ. The model used here has $T_{eff} = 6310$ K, $\log g = 4.3$, $M = 1.2\ M_\odot$, $\alpha = 1.6$, and $v_e = 1$ km s^{-1}. See text for scaling when other values of v_e are used.

FIG. 11.—Critical equatorial rotational velocity for transport of Li under the combined effects of radiative acceleration and circulation, defined as the velocity under which the total transport velocity is always positive (i.e., upward-directed) under the CZ, from the polar axis to the equatorial plane. For v_e below this value, overabundances generated by radiative acceleration can never be reduced by circulation at later times.

larger than that corresponding to the blue edge of the Li gap (see Fig. 1). It will, however, be shown elsewhere (Michaud and Richer 1988) that the depth of convection zones and the mass-temperature relation at their base depend sensitively on the opacity in the stellar atmosphere. This is essentially because the atmosphere determines the adiabat for the whole convection zone. If the atmospheric opacity is increased by a factor of 1.5, α has to be increased from a value of 1.4 to about 1.7 for the depth of the convection zone to remain the same. The atmospheric opacities used here are those of Cox and Stewart (1970). In the temperature range of interest in the atmospheres, these are smaller than the more realistic Kurucz (1979) opacities by a factor of about 1.5. Using more realistic opacities would thus lead to larger values of α for a given depth of convection zones (and thus for a given relation between critical rotational velocity and T_{eff} [cf. Fig. 11]). This will be further discussed in a forthcoming paper.

On the other hand, in order to explain the observed Li abundances in weak G-band giants, it has been suggested by Lambert and Sawyer (1984) that radiative acceleration could, perhaps, through a shielding similar to the one described above, prevent Li from being destroyed while stars evolved up the giant branch. It is worth noting that, on the main sequence, the radiative acceleration only succeeds in shielding Li above $\Delta M/M \approx 10^{-5}$, much less than the 0.6 $M_\odot$ required by Lambert and Sawyer in their model.

b) Lithium and Meridional Circulation

The first conclusion we draw is a conditional one. If the gravitational settling model for the Li gap is confirmed, then it is quite clear from the results presented in § II that, in stars of 7000 K and less, meridional circulation cannot follow the model of T^2 for purely radiative stars. There are stars observed (see Figs. 1 and 2) in the middle of the gap that have both large Li underabundances and rotational velocities much larger than the critical rotational velocities for gravitational settling obtained in § II (between 15 and 7 km s^{-1}, depending on T_{eff} and α).

Actually, even without this assumption, there are already some stars that contradict the abundances expected from transport by meridional circulation. If circulation is as efficient as calculated in § IV, there are a few stars for which the observed Li abundance is larger than should be the case, given the destruction rate caused by meridional circulation at the cluster age.

Consider the combined data of the Pleiades, Hyades, and Coma clusters; Table 2 lists expected and observed Li abundances for the few stars showing significantly larger than expected Li abundances. One field star from Boesgaard and Tripicco (1986*b*) is included, because of its very large v sin i. For such a star not to have been depleted of its Li by more than a factor of 10, one must assume for it an age about 3 times that of the Pleiades, which is unlikely. Calculations were done here with $\alpha = 1.4$; adopting instead a value of 1.6 yields smaller critical velocities. It should be noted that in the case of the two stars of higher effective temperature, the observed v sin i is above the limiting shielding critical velocity given on Figure 11, above which Li depletion occurs despite radiative acceleration [see § V*a* above], although here the choice of α can have

TABLE 2

LITHIUM-RICH F DWARFS WITH HIGH $v \sin i$

Star	$T_{\rm eff}$ (K)	$v \sin i$	Age (yr)	$(v_e)_{\rm crit}$	log $N(\rm Li)_{\rm exp}$	log $N(\rm Li)_{\rm obs}$	Reference
HD 23608	6650	110	7.5×10^7	...	2.52	2.80	1
VB 20	6860	55	8×10^8	...	−4.53	3.29	2
TR 49	6890	50	8×10^8	...	−2.77	2.69	3
			1×10^8	...	2.75	...	
HD 11443	6350	93	5×10^8	...	−1.13	1.92	4
			1×10^8	...	−5.83	...	
VB 6	7110	50	8×10^8	40	−11.65	3.25	2
HD 180777	7110	63	4×10^8	40	−7.17	3.15	5

REFERENCES.—(1) Pleiades star, from Pilachowski, Booth, and Hobbs 1987. (2) Hyades star, from Boesgaard 1987*b*. (3) Coma star, from Boesgaard 1987*a*. (4) Field star, from Boesgaard and Tripicco 1986*b*. (5) Ursa Major star, from Boesgaard, Budge, and Burck 1988.

a great influence. For these stars, circulation is expected to swamp out any effect of diffusion and thus dominate the abundance evolution (cf. § IV). Remembering also that the true v_e can only be equal to or larger than the observed $v \sin i$, one realizes that the list is restrictive, and that at least some of the stars with observed $v \sin i$ near the critical value actually rotate more rapidly. It would seem that meridional circulation has *not* induced the particle transport that one would expect from the calculations of § IV. Note that stars posing a problem to the meridional circulation model all have $T_{\rm eff} > 6800$ K.

Similarly, an argument against any effect of rotation can be made from Table 1. In field stars, there is no correlation between rotation rate and Li underabundance (see § I). Admittedly, however, the sample is relatively small, and there is a possibility of selection effects. Furthermore, this goes against the apparent correlation seen in clusters of ages smaller than 10^9 yr. It is then not a binding argument.

c) *A Possible Alternative to Gravitational Settling*

From Figure 2 (following Boesgaard 1987*b*) we note that rotation is large in the middle of the gap in the Hyades, and that it is significantly larger than in the cooler stars where the Li abundance is normal. This suggests that we may use the results of § IV to determine the Li underabundance that meridional circulation leads to at the ages of the Hyades and UMa, and compare with observations. The model is the following: down to about 7000 K, radiative acceleration dominates Li transport (§ III), so no underabundance can develop; one may even expect overabundances, whose level depends on the equatorial rotational velocity (cf. § III above). As $T_{\rm eff}$ falls below about 6900 K, Li is no longer supported, and meridional circulation carries into the CZ Li-depleted matter. The underabundances depend on the cluster's age, and on effective temperature via the $v \sin i$–$T_{\rm eff}$ relationship adopted. If the effective temperature is further decreased, the average $v \sin i$ becomes so small that depletion is only possible for very old clusters. Since in F stars the bottom of the convection zone is much deeper than the base of the boundary layer of T^2, the meridional circulation velocity field does not depend on the assumed value of turbulent viscosity, so there is no free parameter in the calculations when one uses the observed $v \sin i$ to determine average rotational velocities. Since the exact shape of the $v \sin i$–$T_{\rm eff}$ relationship is known to vary among open clusters (Abt 1970), we use envelopes to measured $v \sin i$ for the Hyades stars of known Li abundance (taken from Boesgaard 1987*b*). The v_e values are chosen for $T_{\rm eff} = 7000$ and 6310 K and rotational velocities for other $T_{\rm eff}$ values are interpolated linearly in between those two values, linearly extrapolated from 6310 to 6200 K, and kept constant below 6200 K. The values used are listed in Table 3, and resulting v_e-$T_{\rm eff}$ relationships are shown with observations in Figure 2.

Results are shown in Figure 12 for ages corresponding to the Hyades (Fig. 12*a*) and UMa (Fig. 12*b*). Expected Li abundance curves and observed abundances are both given. The full line corresponds to case *a* of Table 3, or the most likely rotational velocity envelope for the Hyades. The dashed line corresponds to an increase of the rotational velocity by a factor of 1.5 at $T_{\rm eff} = 6310$ K. The dotted and dash-dot lines correspond to reducing the rotational velocity at $T_{\rm eff} = 7000$ K by factors of 1.5 and 2 respectively.

Consider first case A of Table 3, where the envelope of the observed rotational velocity is assumed for all stars (solid lines on Figs. 2 and 12). The agreement is surprisingly good. In the stars cooler than 6400 K, there is no depletion due to meridional circulation at the age of the Hyades, since the time required to carry matter from the Li-burning region to the convection zone (obtained from Fig. 9) is larger than 7.5×10^8 yr. However, for stars in the gap, the average rotational velocity is larger than the critical v_e obtained by equating $(t_0)_{\rm Li}$ to the corresponding cluster age (recall from § IV that t_0 varies as v_e^{-2}). There is then more and more time, as $T_{\rm eff}$ (and thus the average v_e) is increased, for the matter in the convection zone to be replaced by matter transported by circulation from regions where Li is burned. Equation (14) then leads to a large depletion factor, especially since the replacement time of matter in the convection zone decreases as $T_{\rm eff}$ increases (cf. Fig. 9*d*). Note that v_e appears in an exponential, thus yielding a very strong dependence on the rotation rate. Up to about $T_{\rm eff} = 6800$ K, diffusion is unable to compete with circulation, since the limiting rotational velocity under which gravitational settling is effective was shown to be much smaller than rota-

TABLE 3

$v \sin i$–$T_{\rm eff}$ RELATIONSHIPS

Relationship	7000 K	6310 K
A	70	25
B	70	38
C	47	25
D	35	25

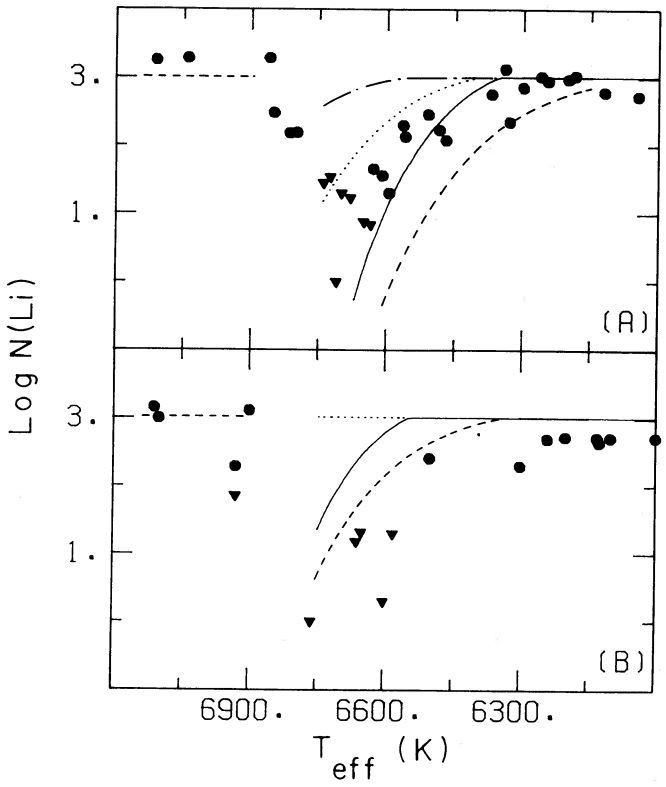

FIG. 12.—Li abundance gaps obtained by considering only the competition between transport by meridional circulation and radiative acceleration (see text). The various gaps were calculated using the v sin i–$T_{\rm eff}$ relationships shown on Fig. 2. (*a*) Gaps obtained at an age of 8×10^8 yr, along with the Hyades data of Boesgaard (1987*b*). (*b*) Gaps obtained at $t = 4 \times 10^8$ yr; includes the UMa data of Boesgaard, Budge, and Burck (1988). Circles represent measured values, and triangles upper limits.

tional velocities used here. However, this critical rotational velocity increases rapidly with $T_{\rm eff}$ (see Fig. 3), and is even larger when radiative acceleration is larger than gravity (cf. § III and Fig. 11). As was discussed at the beginning of this section, for stars hotter than 7000 K, diffusion driven by radiative acceleration can be efficient in "shielding" matter in the convection zone from circulation; this occurs when the radiative acceleration is large enough so that the (upward-directed) diffusion velocity is larger than the downward meridional circulation velocity under the equatorial region of the CZ. For instance, at $T_{\rm eff} = 7100$ K, this occurs for $v_e < 55$ and 25 km s^{-1}, for $\alpha = 1.4$ and 1.6, respectively (see Fig. 10). This large difference comes from the extremely sensitive dependence on α of convection zone mass and from the rapid variation of the diffusion velocity with depth (cf. Fig. 5). This can efficiently keep the Li abundance high at all time in the CZ. The appearance of the gap at $T_{\rm eff} \approx 6900$ K is then due to the rapid increase of depth of the CZ as $T_{\rm eff}$ decreases, via the effect this has on the radiative acceleration and on the ratio of circulation to total diffusion velocity at the base of the CZ.

If one assumes that the envelope of the rotational velocity gives the rotational velocity of the Hyades stars, *one reproduces the observed gap well.* However, the fit deteriorates if a reasonable velocity spread is introduced. Because of the relatively large number of low-velocity points between 6600 and 6900 K, it does not appear plausible that these are all due to projection effects, and that all stars of the Hyades have the same rotational velocity at a given $T_{\rm eff}$. It appears more likely that there is a genuine spread in rotational velocities. Comparing the solid lines to the dash-dot or dotted lines gives an evaluation of the effect of such a spread. Some stars would be expected to have lost their Li, while others should not have suffered any depletion.

Results for UMa are shown in Figure 12*b*. For the observed abundance gap to be reproduced in UMa, the rotational velocities would need to be larger than used here, while observations show that rotational velocities in UMa are not larger than those in the Hyades (cf. Fig. 2*c*), and that observed underabundances are just as large. Since UMa is about half as old as the Hyades, the underabundances should be much smaller than observed.

There are thus three definite objections to the above scenario. *First*, any v sin i–$T_{\rm eff}$ relation is expected to show a certain amount of scatter in v sin i for a given $T_{\rm eff}$, which would show up in observations as vertical scatter in abundances. Yet the gap observed in the Hyades is well defined and shows little vertical scatter. This is not the case in Ursa Major, but one must here recall the rather large uncertainties in effective temperatures (see the discussion in Boesgaard, Budge, and Burck 1988). *Second*, even though UMa is younger than the Hyades and shows about the same v sin i–$T_{\rm eff}$ relationship, it has as large underabundances as the Hyades. *Third*, if competition between transport by meridional circulation and radiative acceleration is responsible for the presence of the observed abundance gaps, one cannot account for the stars listed in Table 2 that do not show the Li underabundances expected from circulation-induced particle transport. In particular, some of the faster-rotating stars with $T_{\rm eff} > 6900$ K should show some Li depletion. Yet, a few Am stars notwithstanding (see Burkhart, Coupry, and Van't Veer 1987), the stars hotter than 6900 K show little Li depletion. We do not discuss Am stars here, since their convection zones are smaller and the radiative acceleration calculations used here do not apply. Furthermore, even in the Hyades, evolutionary effects may start to be important for some stars. It thus appears preferable to discuss Li abundances in Am stars at the same time as their other abundance anomalies, which is outside the scope of the present paper.

d) The Beryllium/Lithium Ratio: A Test of Lithium-burning Models

An observational test of the gravitational settling model has been proposed elsewhere by one of us (Michaud 1987). The meridional circulation model also lends itself to a specific observational test. It involves a comparison of Li and Be abundances. As shown in Figure 10 for a model with $T_{\rm eff} = 6310$ K, the Li/Be ratio reaches a minimum value, which remains constant as the abundance evolution is carried further in time. This minimum value is reached when Be-depleted matter starts arriving in the CZ. As the evolution progresses further, both Li and Be abundances are reduced by the same factor (see the end of § IV for further details). This critical value depends mainly on the relative position of the bottom of the CZ and the positions where Li and Be burn, and thus shows a strong dependence on $T_{\rm eff}$ and α. The Li and Be abundances of course keep on decreasing, but their ratio remains constant. Therefore, this test does not depend on the star's age and so can be applied to field stars for which both Li and Be abundances have been

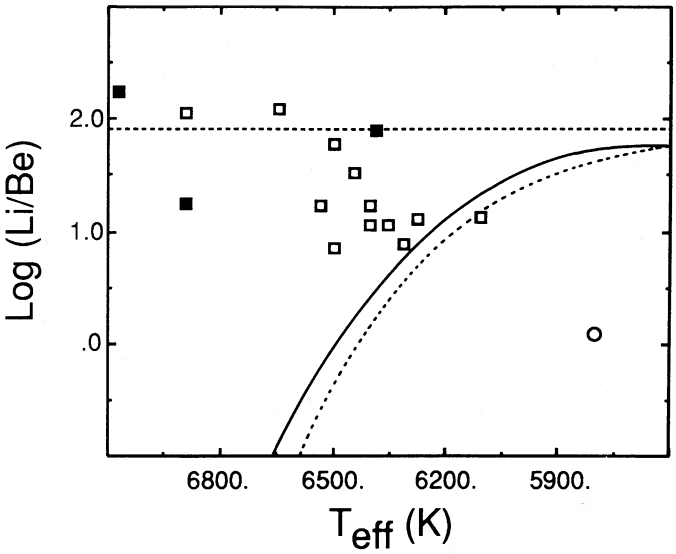

FIG. 13.—Ratio of Li to Be abundances expected from transport by meridional circulation. The curve indicates the ratio attained once both Li and Be have entered the third phase of the abundance evolution (described by eqs. [14] and [15]). It thus represents a lower limit to the Li/Be ratio attainable for a given stellar model. The solid curve corresponds to models with $\alpha = 1.4$, the dotted curve to $\alpha = 1.6$. Field star data are shown (*open symbols*; taken from Wolff, Boesgaard, and Simon 1986), along with a few stars from the Hyades for which both Be and Li abundances have been measured (*filled symbols*; taken from Boesgaard, Heacox, and Conti 1977 and Boesgaard and Tripicco 1986*a*). The Li/Be ratio observed in the Sun is also indicated (*open circle*). The horizontal dashed line indicates the cosmological Li/Be ratio.

measured. Figure 13 shows the observational results, together with the limiting curve. The time evolution of the Li/Be ratio for a star of a given T_{eff} would be given by a vertical path in Figure 13, starting at the initial (cosmological) value at $t = 0$, remaining there until $t = (t_0)_{Li}$, then moving downward and ending up on the curve at $t = (t_0)_{Be}$. Since a given star might not be old enough to have entered the phase of its abundance evolution where Li/Be is constant, this curve must be interpreted as a lower envelope, and clearly no star should fall to the lower right of the curve *if* the evolution of Li and Be abundances is governed by meridional circulation. The Sun clearly does not fit this pattern, which implies that meridional circulation is not responsible for the observed low solar Li abundance. It is actually easy to calculate, given the age and actual rotation rate of the Sun, that the circulation velocity field of T^2 does not lead to any destruction of Li. Turbulence must probably be invoked to explain the Li underabundance in the Sun (Cayrel *et al.* 1984; Baglin, Morel, and Schatzman 1985). There is only one star, with $T_{eff} \approx 6100$ K, lying in the forbidden region. It has a Li/Be ratio lower than the expected value, although using $\alpha = 1.6$ brings the expected Li/Be ratio at this temperature just slightly above the observed value. Observations available at this time do show that all Be-deficient stars are also Li-deficient (see Fig. 8 of Boesgaard and Lavery 1986). Although no conclusion can be drawn at the present time, it seems that this test should be applied to more objects and could ultimately lead to excluding some hydrodynamical models. Clearly, more measurements of Be abundances in Li-depleted stars are needed. It would also be interesting to compare this behavior with that expected from the burning of Li and Be by turbulent transport.

e) Hydrodynamical Implications

It is appropriate to recapitulate the hydrodynamical implications of the abundance anomalies observed in F stars. In our opinion, the gravitational settling model is the simplest that has been proposed to explain the Li abundance gap. It explains most naturally the T_{eff} position of the gap, as well as its width, and is based entirely on well-understood physics. However, as emphasized by Michaud (1987), expected underabundances are by a factor of 20 or so at the age of the Hyades. Given the uncertainties and possible effects of mass loss (Michaud 1987), factors of 50–100 could be explained. Underabundances by factors of up to 1000 have, however, recently been proposed by Boesgaard (1987*b*; but see § I above). The confirmation of such low upper limits would be a strong argument against the gravitational settling model formulated by Michaud (1986), as would be a failure to find the expected oxygen underabundances (Michaud 1987) also produced by gravitational settling in this model. One may then have to resort to models implying the destruction of Li by nuclear reactions and subsequent transport in the CZ, as described in § V*b*. The relatively poor correlation between Li underabundance and rotation rate (see § I herein) for $T_{eff} > 7000$ K could be partially explained by the aforementioned shielding of the CZ from Li-depleted material.

An alternative possibility would be the turbulent diffusion model proposed by Thévenin, Vauclair, and Vauclair (1986; see also Vauclair 1988). The observational test described above would help to distinguish between these two alternatives.

Whichever model is finally corroborated by observations will have interesting hydrodynamical implications. If the gravitational settling model is confirmed, it will imply that the meridional circulation model does not apply to F stars having deep convection zones (see also the conclusion of CM). This may not be surprising, since the T^2 calculation of circulation patterns explicitly assumes that the outer stellar regions are completely radiative. This model would also put an upper limit on the turbulent diffusion coefficient below convection zones of stars. (As explained in Tassoul and Tassoul 1988, § III, this is, however, *not* an upper limit on the eddy viscosities.) If, on the other hand, the meridional circulation model is corroborated, it would imply that the T^2 circulation patterns also apply to stars with deep convection zones. It would also imply that there is very little turbulent particle transport in such models. Finally, if the rotationally induced turbulent transport model is confirmed, it would teach us a great deal about the distribution of turbulence in rotating stars. It would have the surprising consequence that the poorly known turbulent transport coefficients adjust themselves to produce the same equivalent particle transport, at the age of the Hyades, as meridional circulation.

In this paper all calculations were done assuming that the presence of a superficial convection zone does not modify the circulation patterns of T^2. It can be shown that in rotating convection zones the anisotropy in the convective velocity distribution (due primarily to the existence of a strong vertical buoyancy force) generates large-scale circulation currents (see § 8.4 of Tassoul 1978). The explicit inclusion of centrifugal and

Coriolis terms in the convective velocity distribution complicates the problem even further. Not surprisingly, completely consistent models of circulation in convection zones are not yet available, but those calculated so far generally consist of one or more closed cells, i.e., the (mechanically driven) circulation patterns are confined to the CZ (see, e.g., Glatzmaier and Gilman 1982; Durney 1987). Although this is usually prescribed as a boundary condition in these calculations, it is a quite reasonable one, since effective viscosities in convection zones are expected to be much larger than in radiative zones. It is then possible that there is no penetration of the convection zone by the *underlying* (thermally driven) meridional circulation. Assuming partial penetration would necessarily lead to some arbitrariness in the calculations. One possible approach would be to apply the surface boundary condition at the base of the CZ. The vertical component of the circulation velocity would then vanish there, and one would obtain very little mixing between radiative and convective zones. However, the boundary between these two zones is not expected to be clearly delineated, owing to the presence of overshooting. If the latter extends at least as deep as the bottom of the boundary layer, considerable mixing could occur. The results obtained here (and in CM) would then probably remain unchanged within a factor of 2, since the vertical component of the circulation velocity below the boundary layer (and thus the mixed zone) would be of the order of that of the T^2 solution (which is identical with the Sweet solution outside the surface and core boundary layers). If, on the other hand, overshooting extends over only a small fraction of the boundary layer, the effect of circulation on He or Li settling could be very small. An accurate determination of this effect would involve the (as yet unknown) amount of overshooting existing below convective zones of main-sequence stars, and would require calculations of new meridional circulation velocity fields in envelope models containing convective zones, rather than in the completely radiative envelopes of T^2. This is outside the scope of the present paper.

We wish to thank J.-L. Tassoul for numerous useful discussions, and S. Balachandran, A. Boesgaard, and C. Pilachowski for communicating their results ahead of publication.

REFERENCES

Abt, H. A. 1970, in *Stellar Rotation*, ed. A. Slettebak (New York: Gordon & Breach), p. 196.
Baglin, A., Morel, P., and Schatzman, E. 1985, *Astr. Ap.*, **149**, 309.
Balachandran, S. 1987, *Bull. AAS*, **19**, 1128.
Balachandran, S., Lambert, D. L., and Stauffer, R. 1987, preprint.
Boesgaard, A. M. 1987*a*, *Ap. J.*, **321**, 967.
———. 1987*b*, *Pub. A.S.P.*, **99**, 1067.
Boesgaard, A. M., and Budge, K. G. 1988, preprint.
Boesgaard, A. M., Budge, K. G., and Burck, E. B. 1988, *Ap. J.*, **325**, 749.
Boesgaard, A. M., Budge, K. G., and Ramsay, M. E. 1988, *Ap. J.*, **327**, 389.
Boesgaard, A. M., Heacox, W. D., and Conti, P. S. 1977, *Ap. J.*, **214**, 124.
Boesgaard, A. M., and Lavery, R. J. 1986, *Ap. J.*, **309**, L49.
Boesgaard, A. M., and Tripicco, M. J. 1986*a*, *Ap. J.* (*Letters*), **302**, L49.
———. 1986*b*, *Ap. J.*, **303**, 724.
Burkhart, C., Coupry, M. F., and Van't Veer, C. 1987, in *IAU Symposium 132, The Impact of Very High S/N Spectroscopy on Stellar Physics*, ed. G. Cayrel and M. Spite (Dordrecht: Reidel), p. 401.
Cayrel, R., Cayrel de Strobel, G., Campbell, B., and Däppen, W. 1984, *Ap. J.*, **283**, 205.
Charbonneau, P., and Michaud, G. 1988, *Ap. J.*, **327**, 809 (CM).
Cox, A. N., and Steward, J. N. 1970, *Ap. J. Suppl.*, **19**, 243.
Durney, B. R. 1987, in *The Internal Solar Angular Velocity*, ed. B. R. Durney and S. Sofia (Dordrecht: Reidel), p. 235.
Glatzmaier, G. A., and Gilman, P. A. 1982, *Ap. J.*, **256**, 316.
Hobbs, L. M., and Duncan, D. K. 1987, *Ap. J.*, **317**, 796.
Hobbs, L. M., and Pilachowski, C. 1986*a*, *Ap. J.* (*Letters*), **309**, L17.
———. 1986*b*, *Ap. J.* (*Letters*), **311**, L37.
Keller, H. B. 1974, *SIAM J. Numer. Anal.*, **11**, 305.
Kurucz, R. L. 1979, *Ap. J. Suppl.*, **40**, 1.
Lambert, D. L., and Sawyer, S. R. 1984, *Ap. J.*, **283**, 192.
Landau, L. D., and Lifshitz, E. M. 1959, *Fluid Mechanics* (New York: Pergamon), p. 22.
Lebreton, Y., and Maeder, A. 1986, *Astr. Ap.*, **161**, 119.
Martel, G. 1974, Internal Rept., Université de Montréal.
Michaud, G. 1985, in *Solar Neutrinos and Neutrino Astronomy*, ed. M. L. Cherry, K. Landé, and W. A. Fowler (New York: AIP), p. 75.
———. 1986, *Ap. J.*, **302**, 650.
———. 1987, in *IAU Colloquium 108, Atmospheric Diagnostics of Stellar Evolution: Chemical Peculiarity, Mass Loss, and Explosion*, ed. K. Nomoto (Tokyo: Springer Verlag), in press.
Michaud, G., Fontaine, G., and Beaudet, G. 1984, *Ap. J.*, **282**, 206.
Michaud, G., and Richer, J. 1988, in preparation.
Paquette, C., Pelletier, C., Fontaine, G., and Michaud, G. 1986, *Ap. J. Suppl.*, **61**, 177.
Pelletier, C. 1986, Ph.D. thesis, Université de Montréal.
Pilachowsky, C. A., Booth, J., and Hobbs, L. M. 1987, *Pub. A.S.P.*, **99**, 1228.
Schatzman, E. 1977, *Astr. Ap.*, **56**, 211.
Spite, F., Spite, M., Peterson, R. C., and Chaffee, F. H., Jr. 1987, *Astr. Ap.*, **171**, L8.
Spite, M., Maillard, J. P., and Spite, F. 1984, *Astr. Ap.*, **141**, 56.
Tassoul, J.-L. 1978, *Theory of Rotating Stars* (Princeton: Princeton University Press).
Tassoul, J.-L., and Tassoul, M. 1982, *Ap. J. Suppl.*, **49**, 317 (T^2).
Tassoul, M., and Tassoul, J.-L. 1988, *M.N.R.A.S.*, in press.
Thévenin, F., Vauclair, S., and Vauclair, G. 1986, *Astr. Ap.*, **166**, 216.
VandenBerg, D. A., and Bridges, T. J. 1984, *Ap. J.*, **278**, 679.
Vauclair, S. 1987, in *IAU Symposium 132, The Impact of Very High S/N Spectroscopy on Stellar Physics*, ed. G. Cayrel and M. Spite (Dordrecht: Reidel), p. 463.
———. 1988, preprint.
Vauclair, S., Vauclair, G., Schatzman, E., and Michaud, G. 1978, *Ap. J.*, **223**, 567.
Wolff, S. C., Boesgaard, A. M., and Simon, T. 1986, *Ap. J.*, **310**, 360.

P. CHARBONNEAU and G. MICHAUD: Département de Physique, Université de Montréal, C.P. 6128, succursale A, Montréal, Québec, Canada H3C 3J7